Metrol. Meas. Syst., Vol. 31 (2024) No. 3, pp. 465–480
DOI: 10.24425/mms.2024.150290

PAN POLSKA AKADEMIA NAUK

METROLOGY AND MEASUREMENT SYSTEMS
Index 330930, ISSN 0860-8229
www.metrology.wat.edu.pl

M&MS

ENERGY-EFFICIENT DISTRIBUTED ESTIMATION ALGORITHM FOR WIRELESS SENSOR NETWORKS BASED ON COVARIANCE INTERSECTION WITH EIGENDECOMPOSITION

Przemysław Pasek, Piotr Kaniewski

Military University of Technology, Faculty of Electronics, Gen. S. Kaliskiego 2, 00-908 Warsaw, Poland
(✉ *przemyslaw.pasek@wat.edu.pl*)

Abstract

The paper introduces and assesses the Eigenvalue Covariance Intersection (EVCI) algorithm for data fusion in Wireless Sensor Networks. The EVCI aims to enhance information fusion efficiency, reduce transmitted data, and potentially extend network lifespan. By conducting the eigendecomposition of covariance matrices, the EVCI evaluates the utility of eigenvectors and strategically employs only those positively impacting estimate accuracy. Through simulations and comparisons with the Covariance Intersection (CI) algorithm, the study demonstrates EVCI's ability to maintain accuracy alongside with significant energy savings. The paper provides insights into popular data fusion algorithms, the concept of the EVCI, used formulas, and selected simulation results.

Keywords: wireless sensor networks, data fusion, state estimation, covariance intersection, energy efficiency, data reduction.

1. Introduction

Wireless Sensor Networks (WSNs) have become very popular in various branches of industry, science, business, and everyday life. They can be utilized in numerous applications, such as environmental monitoring, object tracking, health monitoring or surveillance [1–5]. The main benefit of using these solutions is the ability to use small, low-cost sensing nodes that can cover a large area and perform tasks that a single, sophisticated device would not be able to conduct, or its use would be expensive and inefficient [6, 7].

A massive increase in the availability of devices with low-power consumption, relatively high computational capabilities, and long lifespan can be observed on the market [3, 5, 6]. They can measure various parameters, with the most commonly monitored being range, temperature, pressure, humidity, and acidity [1–5, 8].

The indicated features, combined with the ability to exchange data among such sensors and possible scalability, have made WSNs widely used in military applications and in the industrial

Article history: received November 29, 2023; revised March 15, 2024; accepted April 11, 2024; available online July 12, 2024.

sector [9, 10]. Solutions based on WSNs, utilizing both homogeneous and heterogeneous sensors, have been successfully implemented in outdoor as well as indoor applications [11].

Despite the popularity and widespread use of WSNs today, their further development requires solving issues related to, among others, a large amount of processed data, a massive number of devices and communication between them. Furthermore, the problems of effortlessly deploying sensors and, if necessary, expanding the network must be addressed. Solutions to these challenges can be sought in the development of the hardware layer or in the algorithms that are responsible for the operation of the network and analysing information [7, 12].

Especially important challenges that need to be addressed are the need to effectively fuse data from multiple devices and ensuring the most accurate outcome [12, 13]. It is a demanding task in both centralized and decentralized approach. The problem is to find a solution that would not require the exchange of a large amount of data and, consequently, high bandwidth consumption. At the same time, it should ensure high accuracy of the final result. These are needed to make good use of the benefits of the idea of sensor networks and thus gain an advantage over other systems [13]. The problem of finding the optimal solution varies depending on the purpose of the WSN and requires a compromise between limiting the data being transmitted and performance of the system [3, 5].

Each WSN has its constraints resulting mainly from hardware limitations which are caused by small sizes of devices and their low cost. Most sensors are battery powered and have limited energy resources [6, 13, 14]. Therefore, all actions related to the performance of their intended tasks must be energy efficient. It is known that the energy used to emit signals is a heavy load for the sensors and this activity requires more resources than the processing of the received data, and the calculations made on their basis [5, 14]. All redundant processes and operations reduce WSN lifespan, and this is the reason why so much attention should be paid to optimize, in terms of both hardware and software, the power consumption of individual nodes [3, 5, 8, 15–18]. Energy savings can be achieved through various means, such as reducing the frequency of data transmission during periods of low dynamic changes in observed quantities or when the node's battery is nearing depletion, thereby enabling an energy-saving mode [3].

In this paper, we address the challenges mentioned above and introduce a novel data fusion technique which is based on the *Covariance Intersection* (CI) algorithm [19]. In order to limit the amount of transferred data and, in consequence, to make the network more efficient in terms of energy consumption, data selection is performed by each sensor before transmission. It is based on eigendecomposition of the covariance matrix and the assessment of the usefulness of the data. It is conducted by analysing the obtained eigenvalues. In this way, it is possible to significantly reduce transmitted data by omitting values that do not contribute positively to the final result. The proposed selection methodology ensures that the limitation of the shared data does not affect the accuracy of the outcome.

This paper is organized as follows. The problem formulation is described in Section 2. A review of common data fusion techniques is presented in Section 3. In Section 4, the proposed *Eigenvalue Covariance Intersection* (EVCI) algorithm is described in detail. Selected results of the simulation experiments are included in Section 5, and Section 6 contains concluding remarks.

2. Problem formulation

In the following sections, we address the problem of fusing data from sensors within a WSN. The considered network comprises n interconnected devices, collaborating to exchange information and process data for generating a unified output.

Each sensor node determines the state of the observed object, which is characterized by two distinct equations: a dynamics model and an observation model [20, 21]. Mathematically, in a discrete-time domain they are expressed as follows [20]:

$$\mathbf{x}_i(k+1) = \mathbf{\Phi}_i(k+1, k)\,\mathbf{x}_i(k) + \mathbf{w}_i(k), \tag{1}$$

$$\mathbf{z}_i(k) = \mathbf{h}_i[\mathbf{x}_i(k), k] + \mathbf{v}_i(k), \tag{2}$$

where: $\mathbf{x}$ – state vector, $\mathbf{\Phi}$ – transition matrix, $\mathbf{w}$ – vector of random process disturbances, $\mathbf{z}(k)$ – vector of acquired measurements at time k, $\mathbf{h}$ – a non-linear observation function and $\mathbf{v}_i$ – measurement noise [20]. All of the presented quantities refer to the i-th sensor in the considered network.

Each node, as a result of individual measurements and estimations often facilitated by algorithms such as the Kalman filter, possesses information in the form of a state vector, and an associated covariance matrix.

The data fusion process typically involves a linear combination of all the data from each sensor to calculate a global state vector $\mathbf{x}$. For n nodes the following formula is used [19]:

$$\mathbf{x} = \mathbf{W}_1\hat{x}_1 + \mathbf{W}_2\hat{x}_2 + \ldots + \mathbf{W}_n\hat{x}_n = \sum_{i=1}^{n} \mathbf{W}_i\hat{x}_i, \tag{3}$$

and a corresponding global covariance matrix $\mathbf{P}$:

$$\mathbf{P} = \sum_{i=1}^{n}\sum_{j=1}^{n} \mathbf{W}_i\mathbf{P}_{ij}\mathbf{W}_j^T, \tag{4}$$

where $\mathbf{W}_i$ denotes the proper fusion gain and $\mathbf{P}_{ij}$ is a cross-correlation matrix or a covariance matrix when $i = j$.

This conventional approach often overlooks the significance of cross-correlation between variables, making its use less justified in many cases. It is crucial to take into account the fact that usually the value of the cross-correlation is unknown and considering it ensures that the fused data is not only representative but also unbiased, thereby providing reliable insights into the state of the observed quantity [19].

Our goal in this research was to devise a novel algorithm that builds upon existing data fusion methodologies, addressing the challenge of handling unknown cross-correlations. Simultaneously, we aimed to meet the specific demands of Wireless Sensor Networks, where data transmission efficiency is crucial. The proposed algorithm achieves a reduction in data transmitted by the sensors while upholding the accuracy of estimated results.

3. Data fusion techniques

In the following section, examples of typical existing data fusion algorithms are briefly described. To improve clarity and to make the distinctive characteristics of each method readily visible, this section of the article focuses on presenting the relevant dependencies with reference to two data sources. In the presented considerations, the authors refer to the local state vector estimates of two sensors $\hat{x}_1$ and $\hat{x}_2$ and their corresponding covariance matrices $\mathbf{P}_1$ and $\mathbf{P}_2$.

In order to fuse two random variables when the value of the cross-correlation between them is known, using a linear combination of the means, and then determining the value of the covariance is the optimal solution [19]. Although, in the case of lack of knowledge about

cross-correlation such an algorithm will not provide a consistent result. This is the reason why the most common data fusion technique, from which many other algorithms were derived, is the Covariance Intersection [19]. The main motivation for the development of the CI was to provide a solution which yields consistent results regardless of the correlation value.

It is based on the convex combination of the means and covariances in the information space. The idea behind the CI algorithm is to use intersection of the covariance matrices of individual sensor measurements, which represent the uncertainty of the measurement from a particular source [19].

$$\mathbf{P}^{-1} = \omega\mathbf{P}_1^{-1} + (1-\omega)\mathbf{P}_2^{-1}, \tag{5}$$

$$\mathbf{P}^{-1}\hat{x} = \omega\mathbf{P}_1^{-1}\hat{x}_1 + (1-\omega)\,\mathbf{P}_2^{-1}\hat{x}_2. \tag{6}$$

According to the CI algorithm, $\mathbf{P}$ matrix lies within the intersection of the covariance matrices of the fused data. That is why a consistent result of the fusion is always provided, and the value of cross-correlation influences only the amount of the information that can be used. Nevertheless, even without any knowledge about $\mathbf{P}_{12}$, at least a conservative estimate can be obtained [19].

Other popular data fusion techniques are usually modifications of the Covariance Intersection algorithm. Since, it has some flaws in certain scenarios, some improvements which would eliminate them were developed.

In [22] a fast non-iterative algorithm called Fast Covariance Intersection was proposed. Its main assumption is an attempt to reduce numerical effort of finding weighting coefficients, since obtaining proper values of them for optimal, in MMSE sense, fusion result requires iterative minimization of the traces (or determinants) of covariance matrices.

In [24] another approach to combine *probability density functions* (PDFs), which represent estimates of certain quantity, called *ellipse intersection* (EI) was proposed. The main reason for the search for a new method was a desire to find a tighter covariance than that achieved by the previous methods. It uses ellipsoids to show the possible values for each estimate, and then it finds a common ellipsoid that includes the best possible combined estimate while considering the different information and uncertainties from each source. While the CI algorithm assumes that the true estimate lies within the intersection of the individual ellipsoids, EI considers both shared information and compromise mean to create a new ellipsoid that balances the estimates' information. In terms of visualisation, CI's result is the intersection of the original ellipsoids, while EI's result is a new ellipsoid that considers both estimates' information [24, 25].

Thorough analysis of the above algorithms showed that the results obtained with the CI are too conservative and may contribute to less accurate estimates. As for the EI, which provides more tight results, there is a risk that the consistency will not be achieved in some cases. Based on these observations, a new algorithm called the *Inverse Covariance Intersection* (ICI) was proposed in [26, 27]. It provides a new ellipsoid that wraps around tightly the overlapping region of the original ones, and it does that by considering the ellipsoids of the inverse covariance matrices.

4. Eigenvalue Covariance Intersection data fusion algorithm

The algorithms discussed earlier provide means to derive estimations for monitored quantities within a sensor network, contributing to varying degrees of accuracy. However, most of these algorithms, with the exception of Fast Covariance Intersection, do not directly tackle the challenge of prolonging device lifespans by limiting specific resource-intensive operations. Notably, the Fast Covariance Intersection algorithm introduces a non-iterative weight determination method, offering a modest reduction in computational operations. This, in turn, translates to a reduction in the energy

consumption during the data fusion process. Building upon the insights discussed earlier, where the energy-intensive nature of signal emissions for data transfer between sensors was highlighted, a strategy that mitigates the need for extensive data exchange among devices was sought to be devised. This approach was designed to achieve a twofold objective: to reduce the energy burden associated with data transmission and, simultaneously, to uphold the accuracy of estimation results.

The core motivation driving the development of the EVCI algorithm revolves around optimizing data exchange between sensors. Recognizing that vital information about the observed parameter's state resides within the local state vector of each sensor and its corresponding covariance matrix, the traditional approach involves interchanging these quantities among sensors. They are obtained using local estimation algorithms in the form of, for example, the Kalman filter or its modifications. Interchange of the mentioned information lays the groundwork for achieving possibly uniform state estimates across the sensor network, enabling a comprehensive understanding of the observed variables.

The unique aspect of the proposed algorithm is its distinctive data selection strategy. Rather than exchanging all available data, the algorithm evaluates the relevance of data before transmission. By doing so, it eliminates the burden of unnecessary data transfer, streamlining the communication process and significantly reducing the energy expenditure associated with data exchange. In consequence, the efficiency and sustainability of the sensor network is elevated by optimizing energy consumption.

It is worth pointing out that employing local state estimation through Kalman filtering results in the loss of higher statistical moments, considering only the mean and covariance of the observed variables. In this context, the proposed EVCI algorithm does not compromise the transmission of this information to other nodes. However, if other local estimation algorithms like *particle filters* (PF) were used in the nodes, data fusion using the EVCI algorithm would restrict the retention of this information. In situations where preserving this data is essential, it is advisable to refrain from using the proposed data fusion algorithm. Nevertheless, while these statistics may offer additional insights into the data distribution, many sensor network applications prioritize accurate estimation of state variables with minimal computational and communication resources.

Another issue associated with using Kalman filtering is the requirement to assume a Gaussian distribution for the observed values, which serves as the foundation for this category of filtering algorithms. When heavy-tailed distributions are encountered, extreme values and outliers are present, and the use of Kalman filtering may not be appropriate. Consequently, the EVCI algorithm is not applicable, as it would result in the loss of higher-order moments. Nonetheless, in many sensor network scenarios a multivariate Gaussian distribution is present, making it a suitable foundation for the algorithm's development. This holds true for various applications such as radar localization networks, position estimation in unmanned aerial vehicle swarms, as well as distributed acoustic sensing and soil monitoring networks [8].

4.1. Data reduction method

The data reduction method is presented within the context of two cooperating devices marked as $N1$ and $N2$, both observing the same quantity. Following the estimation of their respective states via the local Kalman filters, these modules initiate the exchange of crucial data with their neighbouring counterparts (in this scenario, with each other). At the heart of this method lies the eigendecomposition of the covariance matrix, yielding eigenvectors and corresponding eigenvalues:

$$\mathbf{P}_1 = \mathbf{U}_1 \mathbf{\Lambda}_1 \mathbf{U}_1^T = \sum_{k=1}^{n} \mathbf{u}_{1k} \lambda_{1k} \mathbf{u}_{1k}^T. \tag{7}$$

The matrix $\mathbf{U}_1$ contains n columns with eigenvectors $\mathbf{u}_{1k}$, while the diagonal matrix $\mathbf{\Lambda}_1$ holds eigenvalues λ_{1k}. The pivotal criterion employed for selecting the data to be shared among nodes centers on the evaluation of individual eigenvalues. This process of eigenvalue assessment enables the algorithm to make informed decisions about data transmission, ensuring that only the most relevant information is exchanged between the nodes.

The eigenvalues are systematically organized in a non-increasing order. Within this sorted list, they are then divided into two distinct groups:

- The first group encompasses eigenvalues λ_{1k}, where k ranges from 1 to m, and these eigenvalues satisfy the condition $\lambda_{1k} \geq \lambda_t$. Here, λ_t represents a defined threshold value.
- The second group comprises eigenvalues characterized by $\lambda_{1k} < \lambda_t$.

In parallel with this eigenvalue categorization, the corresponding column eigenvectors $\mathbf{u}_{1k}$, are also sorted in the identical order. Building upon the preceding division into two distinctive subgroups, we can express the covariance matrix $\mathbf{P}_1$ as the summation of decomposition outcomes associated with both the larger and smaller eigenvalues:

$$\mathbf{P}_1 = \mathbf{P}_{1r} + \mathbf{P}_{1a} = \mathbf{U}_{1r}\mathbf{\Lambda}_{1r}\mathbf{U}_{1r}^T + \mathbf{U}_{1a}\mathbf{\Lambda}_{1a}\mathbf{U}_{1a}^T. \tag{8}$$

Significant eigenvalues, denoting heightened uncertainty in the specific distribution of the random variable, are omitted from transmission to neighbouring nodes. These high-value components offer marginal enhancements to the fusion accuracy. Consequently, in the relationship (20), this subgroup is designated with the index r signifying *rejected* elements in the data selection process. Meanwhile, the remaining part, signifying the *accepted* data, is denoted with the letter a. Therefore, only the second part of the sum above is transmitted. It can be presented in the following form:

$$\mathbf{P}_{1a} = \mathbf{U}_{1a}\mathbf{\Lambda}_{1a}\mathbf{U}_{1a}^T = \mathbf{U}_{1a}\sqrt{\mathbf{\Lambda}_{1a}}\sqrt{\mathbf{\Lambda}_{1a}}\mathbf{U}_{1a}^T = \left(\mathbf{U}_{1a}\sqrt{\mathbf{\Lambda}_{1a}}\right)\left(\mathbf{U}_{1a}\sqrt{\mathbf{\Lambda}_{1a}}\right)^T. \tag{9}$$

A state vector and a selected, properly prepared part of the covariance matrix are sent. Thus, a dataset $\left\{\mathbf{x}_1, \mathbf{U}_{1a}\sqrt{\mathbf{\Lambda}_{1a}}\right\}$ is transferred. Considering that the state vector $\mathbf{x}_1$ comprises n elements, the matrix $\mathbf{U}_{1a}\sqrt{\mathbf{\Lambda}_{1a}}$ possesses n rows and $n-m$ columns, resulting in a total transmission of $n + n\,(n-m)$ numbers.

Neighbouring node $N2$ receives the data $\left\{\mathbf{x}_1, \mathbf{U}_{1a}\sqrt{\mathbf{\Lambda}_{1a}}\right\}$. To process this information, it initiates a series of steps. First, the received matrix $\mathbf{U}_{1a}\sqrt{\mathbf{\Lambda}_{1a}}$ undergoes *Singular Value Decomposition* (SVD) as follows:

$$[\mathbf{U}_{1\text{null}}, \mathbf{S}, \mathbf{V}] = svd\left(\mathbf{U}_{1a}\sqrt{\mathbf{\Lambda}_{1a}}\right). \tag{10}$$

This decomposition, represented as $\mathbf{U}_{1a}\sqrt{\mathbf{\Lambda}_{1a}} = \mathbf{U}_{1\text{null}}\mathbf{S}\mathbf{V}^T$, allows to extract the columns of matrix $\mathbf{V}$ that correspond to zero singular values in $\mathbf{S}$. These columns collectively form an orthonormal basis of vectors known as $\mathbf{U}_{1\text{null}}$, which characterizes the zero subspace of the $\mathbf{U}_{1a}\sqrt{\mathbf{\Lambda}_{1a}}$ matrix, essentially representing the kernel of this transformation.

Subsequently, the $N2$ node that received the data reconstructs the matrix $\mathbf{P}_1$ using two components: $\mathbf{P}_{1\text{null}}$, which replaces the missing data from the matrices $\mathbf{P}_{1r}$, and $\mathbf{P}_{1a}$. The reconstructed matrix is denoted by $\widetilde{P}_1$ and the process is defined by:

$$\widetilde{P}_1 = \mathbf{P}_{1\text{null}} + \mathbf{P}_{1a} = \mathbf{U}_{1\text{null}}\mathbf{\Lambda}_{1\text{null}}\mathbf{U}_{1\text{null}}^T + \left(\mathbf{U}_{1a}\sqrt{\mathbf{\Lambda}_{1a}}\right)\left(\mathbf{U}_{1a}\sqrt{\mathbf{\Lambda}_{1a}}\right)^T. \tag{11}$$

Metrol. Meas. Syst., Vol. 31 (2024), No. 3, pp. 465–480
DOI: 10.24425/mms.2024.150290

Here, the $\mathbf{\Lambda}_{1\text{null}}$ matrix is diagonal and contains very large values, selected arbitrarily to represent a high level of uncertainty. In theory, these values should be infinitely large, but in practice, large finite numbers are assumed.

Finally, the module performs data fusion using the reconstructed matrix and its local covariance matrix, as well as the received data vector $\mathbf{x}_1$ and $\mathbf{x}_2$. The fusion equations are given by:

$$\hat{P}_2 = \left(\widetilde{P}_1^{-1} + \mathbf{P}_2^{-1}\right)^{-1}, \tag{12}$$

$$\hat{x}_2 = \hat{P}_2 \left(\widetilde{P}_1^{-1}\mathbf{x}_1 + \mathbf{P}_2^{-1}\mathbf{x}_2\right). \tag{13}$$

These operations enable effective combining data from another node and its own data to generate an improved estimate of the monitored quantity.

Figure 1 visually illustrates the algorithm's concept using error ellipses, which graphically represent covariance matrices. This visualization demonstrates how the algorithm achieves consistent results by rejecting high-uncertainty components and replacing them with infinite values. As can be seen, despite reducing information, the fused data (red ellipsoid) remains consistent and similar to the conventional data fusion result, emphasizing the algorithm's capacity to enhance network efficiency without compromising data accuracy.

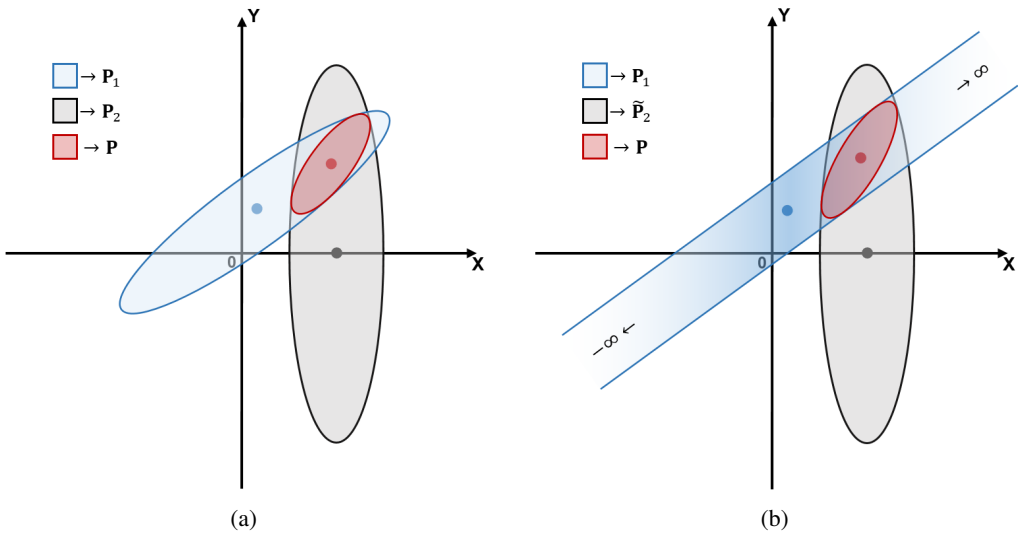

Fig. 1. Comparison of the basic CI algorithm (a) and the EVCI data fusion algorithm (b).

The algorithm's functionality is depicted using a pseudocode below. It illustrates the operations involved in the EVCI algorithm and the information exchange between two sensors. Demonstrating a single iteration of the data fusion process, it begins with data filtration in $N1$, followed by data selection, transmission, reception in $N2$, data reconstruction, and ultimately, data fusion to attain a global state estimate. Figure 2 presents the key operations in individual nodes described in the article. The remaining pseudocode, which is analogous to the one already presented for the other node, has been replaced with dots.

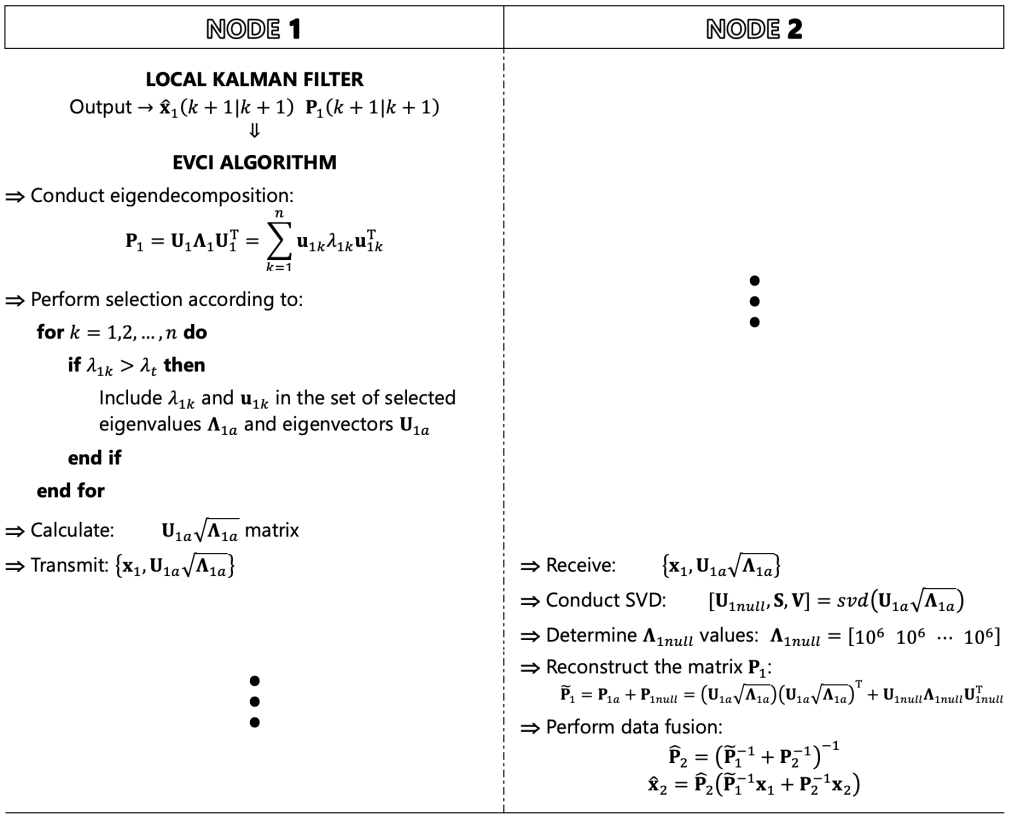

Fig. 2. Pseudocode of the EVCI algorithm depicting the data exchange process between two nodes, culminating in data fusion to obtain a global state estimate at Node 2.

5. Simulation results

To assess the effectiveness of the proposed data fusion algorithm, a series of simulative experiments were conducted. The simulations serve the dual purpose of demonstrating the utility of the algorithm in data fusion and comparing it with a fundamental method used for the same purpose, the CI algorithm. This chapter comprises two primary sections. One section delves into the fundamental properties of the EVCI algorithm under various simulation conditions, while the other highlights the advantages of employing the EVCI and the resulting benefits in terms of data transmission efficiency.

5.1. EVCI algorithm evaluation and comparison with the CI

Our approach to algorithm evaluation mirrors the methodology commonly employed for assessing algorithms of a similar class. A simplified scenario featuring a pair of collaborating sensors, both focused on observing a single object, was assumed. These sensors perform measurements, engage local estimation algorithms, and conduct internal calculations to deliver values characterizing the observed object. The next phase involves sharing these datasets, which leads to the calculation of an overall estimate for the object's state through the fusion process.

For the purpose of this study, we concentrate on sensors that measure distances to track an object's movement. With measurements from a single sensor, the object's three-dimensional position remains indeterminable. However, for the sake of simulation, we presume that within a broader network – whose structure and properties have been deliberately omitted in this analysis – both sensors possess knowledge regarding the object's coordinates. Each sensor maintains its own state vector and covariance matrix, representing its unique perspective on the object's state.

The sensors used in this investigation are *Ultra-Wideband* (UWB) modules, characterized by high-precision distance measurements. It can be assumed that the typical measurement accuracy of commercially available solutions is approximately 2.5 cm [28]. Nonetheless, as part of the simulation, we mimic scenarios where various factors contribute to an escalation of errors. Such factors include disturbances in electromagnetic wave propagation or shifts in network geometry as the object's position relative to the sensors changes. These unpredictable situations generate datasets with random errors, some close to the nominal device accuracy, and others exceeding this threshold due to the aforementioned operational obstacles. It is worth mentioning that in real-world applications, sensor failures can occur. Reducing the transmitted data from a malfunctioning sensor can conserve energy and maintain overall system integrity. This is the key advantage of the EVCI algorithm: it allows for selective reduction of data, minimizing the impact of erroneous information on the fusion outcome. While a broken sensor's inaccuracies may have less influence on the overall accuracy due to the knowledge about the covariance matrix, it remains prudent to avoid unnecessary data transmission in such scenarios.

The local data from the sensors undergo data fusion through both CI and EVCI algorithms. Notably, when using the proposed EVCI algorithm, we introduce varying reduction thresholds to investigate their impact on the fusion outcome. Given that our considerations maintain equal weights for information originating from both sensors and that they transmit the complete state vector and covariance matrix, the global estimate obtained using the CI algorithm is identical for both sensors. However, the fusion outcomes yielded by the EVCI algorithm manifest a more individual nature. This distinction arises because different datasets may be transmitted to each sensor. For example, one sensor might relay the full covariance matrix, while the other may transmit a subset of the reduced eigenvectors. As a consequence, the fusion results may exhibit slight differences between the sensors, and, for this reason, we present them from both sensors for a comprehensive evaluation of their performance.

In the subsequent simulations, the process was initiated by defining true values that describe the observed object. It was assumed that the position of the object of interest is tracked, therefore the state vector $\mathbf{x}$ and the covariance matrix $\mathbf{P}$ of filtration errors have the following forms:

$$\mathbf{x} = \begin{bmatrix} x & y & z \end{bmatrix}^T, \tag{14}$$

$$\mathbf{P} = \operatorname{diag}\begin{bmatrix} P_x & P_y & P_z \end{bmatrix}^T. \tag{15}$$

Subsequently, a dataset consisting of k samples, reflecting the local estimations from both sensors, was generated. These local estimations encompassed state vectors with predefined error values characteristic of UWB sensors. In parallel, the associated filtration error covariance matrices were generated.

Conducted simulations aimed to serve as a benchmark for the EVCI algorithm. The generated dataset was intentionally tailored to mimic the aforementioned real-world scenarios, which included substantial measurement uncertainties.

Figure 3 provides a comprehensive overview of the results, showcasing the *root square error* (RMSE) values. In order to study distinctions in the outcomes and efficiency of the EVCI to adapt to diverse situations, we explored two different reduction thresholds.

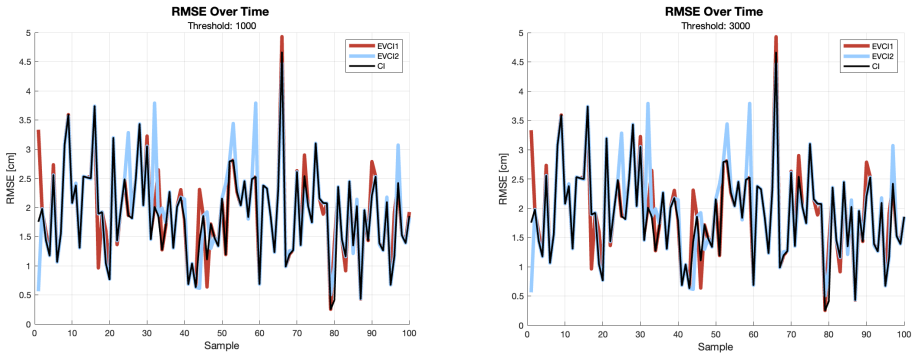

(a) (b)

Fig. 3. RMSE values comparison for the CI and EVCI algorithms for the smaller eigenvalue reduction threshold (a) and for the bigger eigenvalue reduction threshold (b).

RMSE value for the k-th sample is calculated as follows [29]:

$$\mathrm{RMSE}_a(k) = \sqrt{\frac{1}{n}\left(\hat{x}_a(k) - \mathbf{x}(k)\right)^T \left(\hat{x}_a(k) - \mathbf{x}(k)\right)}. \tag{16}$$

Symbol a indicates the algorithm used for calculations (CI/EVCI) and $\hat{x}_a$ denotes the state vector estimated with the a algorithm. The n quantity is the number of the state vector elements.

The results obtained using the EVCI closely match those from the CI, even when adjusting the reduction threshold. This suggests that the choice of threshold had a limited impact on RMSE in the tested scenario.

These findings are reinforced by the Z-component position curves (Fig. 4), which show minor deviations between the utilized algorithms. The results at both reduction thresholds exhibit slight differences, but these deviations do not significantly affect the overall understanding of the observed object.

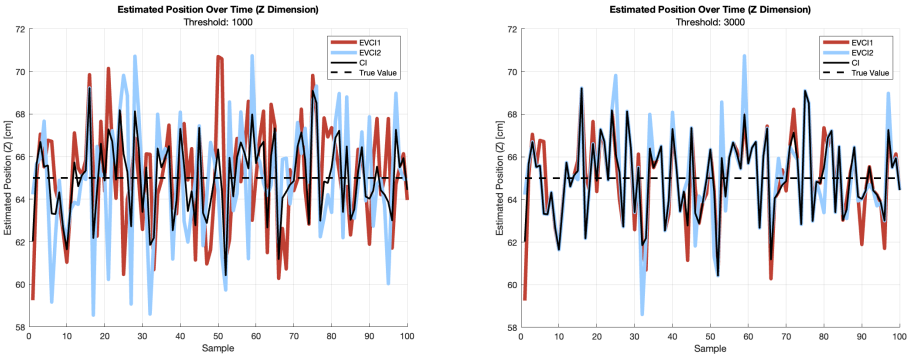

(a) (b)

Fig. 4. The z values comparison of the CI and EVCI algorithms for the smaller eigenvalue reduction threshold (a) and for the bigger eigenvalue reduction threshold (b).

Metrol. Meas. Syst., Vol. 31 (2024), No. 3, pp. 465–480
DOI: 10.24425/mms.2024.150290

In Fig. 5 the estimated values of the Z-component were presented in the form of a graphical representation of the results distribution. It includes statistical information about the dataset's central tendency and spread.

The boxes in the figures above represent the *interquartile range* (IQR), which is the range between the 25th percentile and the 75th percentile of the data. It shows the middle 50% of the data. Red line inside each box represents the median, which is the 50th percentile of the data. The whiskers extend from the edges of the box to the minimum and maximum values within a range, which is defined as 1.5 times the IQR. Red crosses beyond the whiskers are data points which are considered outliers.

Figure 5 reveals that the coordinate values obtained by both algorithms share similar distributions. They illustrate that the range of errors, as well as their median values, align closely between the two algorithms, regardless of the specific sensor or the chosen reduction threshold.

Figure 6 provides a comprehensive view of the three-dimensional object position estimation results. When using a higher reduction threshold, the outcomes closely resemble those of the CI method. With a smaller threshold, although they differ slightly, the errors' distribution and range remain within reasonable limits compared to the CI.

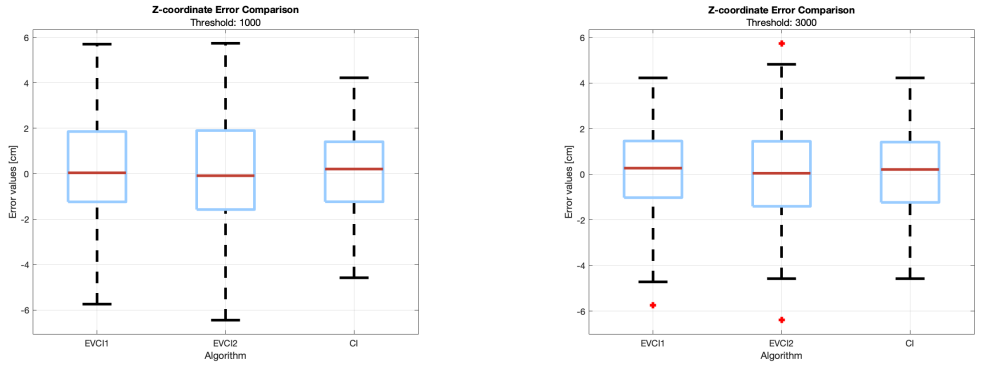

(a) (b)

Fig. 5. Distribution of the Z-component obtained with the CI and EVCI algorithms for the smaller eigenvalue reduction threshold (a) and for the bigger eigenvalue reduction threshold (b).

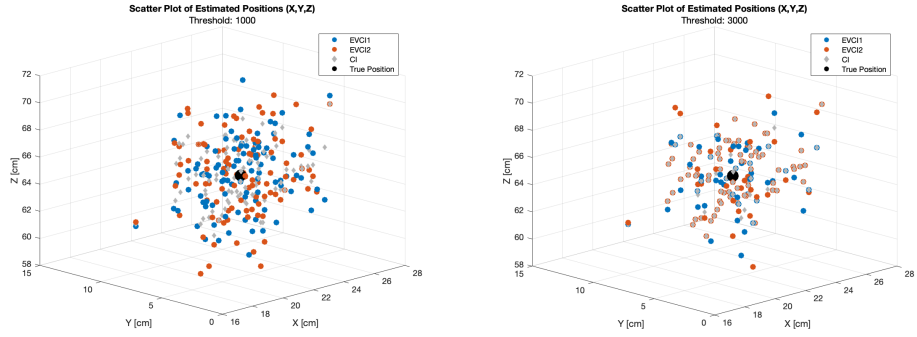

(a) (b)

Fig. 6. Position in three dimensions of the observed object obtained with the CI and EVCI algorithms for the smaller eigenvalue reduction threshold (a) and for the bigger eigenvalue reduction threshold (b).

5.2. Data reduction

The second part of simulation tests focused on exploring potential for reducing unimportant or less critical data with regard to estimation accuracy. Simulations similar to those in the previous section were carried out and the results were examined. In one of these simulation scenarios, the number of observed parameters describing the tracked object was increased to nine. This expansion could include additional variables such as velocity and acceleration or it could be assumed that multiple objects were tracked, though the specific application context was not primary concern in our research. The purpose of this operation was to illustrate that as the state vector grows, the number of error-prone parameters may also increase. This, in turn, highlights the potential for achieving data transmission savings.

Figures 7 and 8 provide a summary of our results, focusing on data from a single sensor (in this case, Sensor no. 1). The first column illustrates RMSE errors, following the same calculation approach as described earlier. Tracking these values allows to observe changes and the growth of estimation errors as data reduction is applied. In the middle column, the number of reduced eigenvectors is shown, indicating the data eliminated prior to transmission. The third column outlines the volume of data transmitted using both CI and EVCI algorithms. Subsequent rows in the figures present results for various data reduction threshold values.

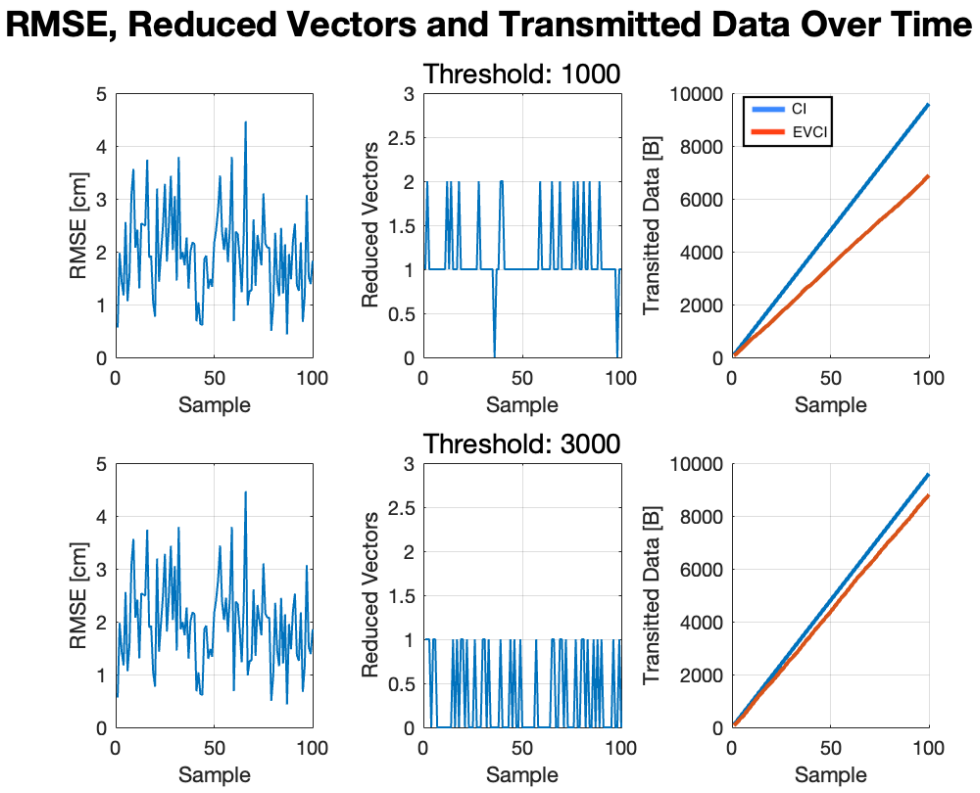

Fig. 7. Comparison of the CI and EVCI algorithms for a three-element state vector with varying eigenvalue reduction thresholds, depicting RMSE values and the amount of data reduced.

Metrol. Meas. Syst., Vol. 31 (2024), No. 3, pp. 465–480
DOI: 10.24425/mms.2024.150290

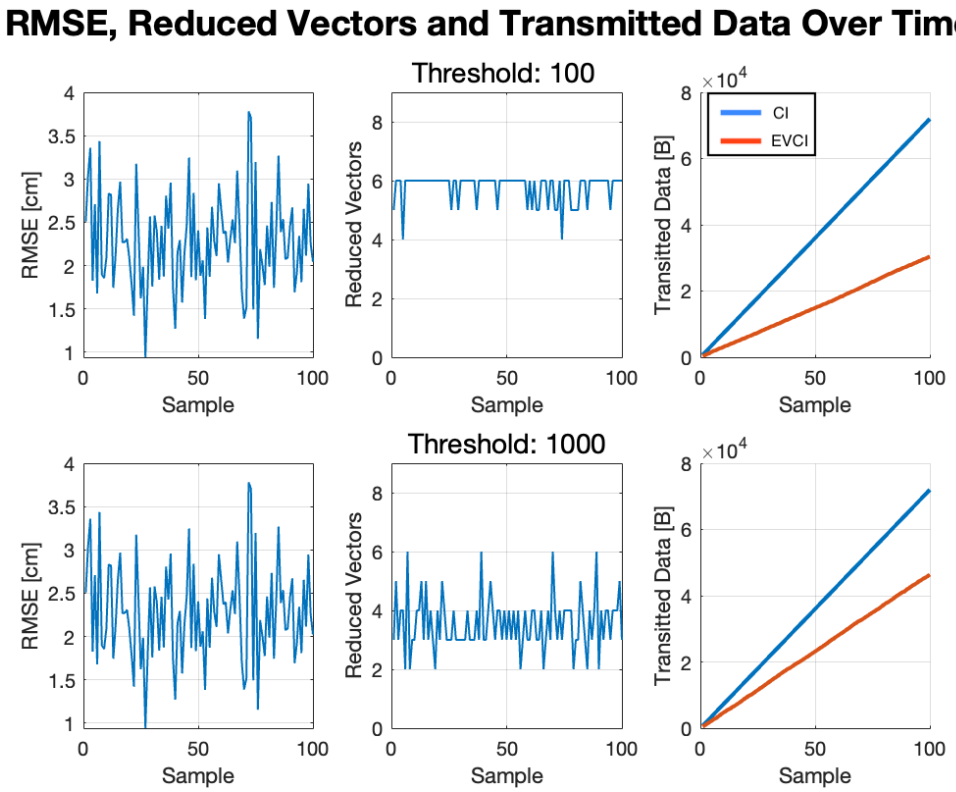

Fig. 8. Comparison of the CI and EVCI algorithms for a nine-element state vector with varying eigenvalue reduction thresholds, depicting RMSE values and the amount of data reduced.

The amount of data transmitted by the sensor was estimated under the assumption that each element in the state vector and the covariance matrix is stored in the device memory as a double-precision floating-point variable (*double*), typically occupying 8 bytes. The following calculations were performed:

$$D_{\mathrm{CI}} = k\left(n + n^2\right) \cdot 8 \text{ B}, \tag{17}$$

$$D_{\mathrm{EVCI}} = \sum_{i=1}^{k} \left(n + n\left(n - m_i\right)\right) \cdot 8 \text{ B}, \tag{18}$$

where D – all the transmitted data, n – the number of observed quantities (number of state vector elements) and m_i – the number of reduced eigenvectors in the i-th simulation step.

As can be seen in the graphs presenting the amount of data transmitted by the sensor, in some scenarios (such as in Fig. 8), where individual elements of the state vector have high uncertainties, a substantial reduction in transmitted data is achievable. Crucially, it does not significantly deteriorate the accuracy of the global estimate obtained as a result of the fusion. This can be observed on the basis of the presented RMSE error curves, which do not differ from each other, despite different reduction levels arising from distinct threshold values.

The results clearly demonstrate that a 50% reduction in data transmission, as compared to the traditional CI algorithm, can be accomplished without compromising estimation accuracy.

Furthermore, it is noteworthy that the greater the number of quantities in the state vector, the more significant the potential for achieving data savings. In extensive sensor networks, the likelihood of inaccurate estimates of observed values is heightened, requiring greater resources to uphold network integrity and precision. This elevated risk of sensor malfunction and measurement inaccuracies underscores the criticality of reducing transmitted data. Moreover, in networks exposed to area interference or intentional jamming, the volume of inaccurate information may escalate considerably. As sensor networks scale up, it is expected that the proportional increase in data reduction will lead to a potentially more advantageous ratio of reduced data to the number of sensors, indicating improved efficiency with larger network sizes.

6. Conclusions

This paper has addressed the issue of data fusion in wireless sensor networks. After exploring the existing methods, the authors proposed their own solution called the *Eigenvalue Covariance Intersection* (EVCI), rooted in the Covariance Intersection. The motivation behind this algorithm was an attempt to minimize data transmission among devices to optimize energy consumption in networks while maintaining the accuracy of the global estimate of observed parameters.

The authors introduced the method for extracting values from the transmitted dataset that would not significantly contribute to the final estimate due to their substantial error. This data selection relies on the eigendecomposition of the local covariance matrix of filtration errors. Analysing eigenvalues enables the rejection of those exceeding an assumed threshold and corresponding eigenvectors. The proposed solution also outlines a method for recovering the covariance matrix in receiving sensors, enabling effective data fusion.

Simulation studies and the comparative analysis between the EVCI and CI algorithms show the potential to significantly reduce data while preserving accuracy. In certain cases, the authors demonstrated nearly a twofold reduction in transmitted data. The results suggest that in specific applications, particularly in wide networks monitoring numerous parameters, substantial energy savings can be achieved with a similar level of errors in the final estimate.

In future works, in-depth simulation research and testing of the algorithm in specific application scenarios are planned. The authors' current efforts focus on implementing the EVCI algorithm in a swarm of *unmanned aerial vehicles* (UAVs), a unique form of sensor network. In such networks, each UAV shares its navigation data with others to provide them with situational awareness and develop a global state estimate. What is more, it is crucial to minimize energy consumption to extend the lifespan of the nodes. Furthermore, the authors aim to explore the optimal reduction threshold selection, considering both the degree of reduction and result accuracy.

Acknowledgements

This work was supported by the Military University of Technology, Poland, under research project UGB 22-752.

References

[1] Ammari, M. (Ed.) (2014). *The Art of Wireless Sensor Networks: Volume 1: Fundamentals*. Springer. https://doi.org/10.1007/978-3-642-40066-7

[2] Ammari, M. (Ed.) (2014). *The Art of Wireless Sensor Networks: Volume 2: Advanced Topics and Applications*. Springer. https://doi.org/10.1007/978-3-642-40009-4

[3] Parimala, K. (Ed.) (2022). *Emerging Trends in Wireless Sensor Networks*. IntechOpen. https://doi.org/10.5772/intechopen.95653

[4] Singh, M. K., Amin, S. I., Imam, S. A., Sachan, V. K., & Choudhary, A. (2018). A Survey of Wireless Sensor Network and its Types. *2018 International Conference on Advances in Computing, Communication Control and Networking (ICACCCN)*, India, 326–330. https://doi.org/10.1109/ICACCCN.2018.8748710

[5] Zheng, J., & Jamalipour, A. (2009). *Wireless Sensor Networks: A Networking Perspective*. John Wiley & Sons. https://ieeexplore.ieee.org/servlet/opac?bknumber=5361027

[6] Suhonen, J., Kohvakka, M., Kaseva, V., Hämäläinen, T., & Hännikäinen, M. (2012). *Low-Power Wireless Sensor Networks: Protocols, Services and Applications*. Springer. https://doi.org/10.1007/978-1-4614-2173-3

[7] Yang S. (2014). *Wireless Sensor Networks: Principles, Design and Applications*. Springer. https://doi.org/10.1007/978-1-4471-5505-8

[8] Gaura, E., Girod, L., Brusey, J., Allen, M., & Challen, G. (2010). *Wireless Sensor Networks: Deployments and Design Frameworks*. Springer. https://doi.org/10.1007/978-1-4419-5834-1

[9] Ali, A. (2020). Military Operations Wireless Sensor Networks based Applications to Reinforce Future Battlefield Command System. *2020 IEEE 23rd International Multitopic Conference (INMIC)*, 1–6. https://doi.org/10.1109/INMIC50486.2020.9318168

[10] Pejanović Đurišić, M., Tafa, Z., Dimić, G., & Milutinović, V. (2012). A survey of military applications of wireless sensor networks. *2012 Mediterranean Conference on Embedded Computing (MECO)*, Montenegro, 196–199. https://ieeexplore.ieee.org/document/6268958

[11] Kaniewski, P., & Pasek, P. (2019). Personal navigation system using ultrawideband technology. *Przegląd Elektrotechniczny*, 95, 136–139. https://doi.org/10.15199/48.2019.11.36

[12] Borges, L. M., Velez, F. J., & Lebres, A. S. (2014). Survey on the characterization and classification of wireless sensor network applications. *IEEE Communications Surveys & Tutorials*, *16*(4), 1860–1890. https://doi.org/10.1109/COMST.2014.2320073

[13] Izadi, D., Abawajy, J. H., Ghanavati, S., & Herawan, T. (2015). A data fusion method in wireless sensor networks. *Sensors*, *15*(2), 2964–2979. https://doi.org/10.3390/s150202964

[14] Chen, Y., Shu, J., Zhang, S., Liu, L., & Sun, L. (2009). Data Fusion in Wireless Sensor Networks. *2009 Second International Symposium on Electronic Commerce and Security*, China, 504–509. https://doi.org/10.1109/ISECS.2009.170

[15] Fan, Z., Jie, Z., & Qian, Y. (2018). A Survey on Wireless Power Transfer based Charging Scheduling Schemes in Wireless Rechargeable Sensor Networks. *2018 IEEE 4th International Conference on Control Science and Systems Engineering (ICCSSE)*, China, 194–198. https://doi.org/10.1109/CCSSE.2018.8724809

[16] Zhaohua, L., & Mingjun, G. (2009). Survey on network lifetime research for wireless sensor networks. *2nd IEEE International Conference on Broadband Network & Multimedia Technology*, China, 899–902. https://doi.org/10.1109/ICBNMT.2009.5347814

[17] Harish, S. V., & Archana, N. V. (2023). Pragmatic Distribution Based Routing Cluster to Improve Energy Efficient Cluster Lifetime for Wireless Sensor Networks. *Metrology and Measurement Systems*, *69*(2), 353–360. https://doi.org/10.24425/ijet.2023.144371

[18] Paś, J. (2023). Issues Related to Power Supply Reliability in Integrated Electronic Security Systems Operated in Buildings and Vast Areas. *Energies*, *16*(8), 3351. https://doi.org/10.3390/en16083351

[19] Julier, S. J., & Uhlmann, J. K. (1997, June). A non-divergent estimation algorithm in the presence of unknown correlations. In Proceedings of the 1997 American Control Conference (Cat. No. 97CH36041) (Vol. 4, pp. 2369–2373). IEEE. https://doi.org/10.1109/ACC.1997.609105

[20] Kaniewski, P. (2010). *Structures, models and algorithms in integrated positioning and navigation systems*. Wyd. WAT.

[21] Kaniewski, P., Gil, R., & Konatowski, S. (2017). Estimation of UAV Position with Use of Smoothing Algorithms. *Metrology and Measurement Systems*, *24*(1), 127–142. https://doi.org/10.1515/mms-2017-0013

[22] Niehsen, W. (2002). Information fusion based on fast covariance intersection filtering. *Proceedings of the Fifth International Conference on Information Fusion*, USA, 901–904 vol. 2. https://doi.org/10.1109/ICIF.2002.1020907

[23] Franken, D., & Hupper, A. (2005). Improved fast covariance intersection for distributed data fusion. *7th International Conference on Information Fusion*, USA. https://doi.org/10.1109/ICIF.2005.1591849

[24] Sijs, J., Lazar, M., & Bosch, P. P. J. V. D. (2010, June). State fusion with unknown correlation: Ellipsoidal intersection. In *Proceedings of the 2010 American Control Conference* (pp. 3992–3997). IEEE. https://doi.org/10.1109/ACC.2010.5531237

[25] Sijs, J., & Lazar, M. (2011). Empirical case-studies of state fusion via ellipsoidal intersection. *14th International Conference on Information Fusion*, USA, 1–8. https://ieeexplore.ieee.org/document/5977578

[26] Noack, B., Sijs, J., Reinhardt, M., & Hanebeck, U. D. (2017). Decentralized data fusion with inverse covariance intersection. *Automatica*, *79*, 35–41. https://doi.org/10.1016/j.automatica.2017.01.019

[27] Noack, B., Sijs, J., & Hanebeck, U. D. (2017, July). Inverse covariance intersection: New insights and properties. In *2017 20th International Conference on Information Fusion (Fusion)* (pp. 1–8). IEEE. https://doi.org/10.23919/ICIF.2017.8009694

[28] PulsON 440 Datasheet/User Guide (2017)

[29] Specht, O. (2023). Method for accuracy assessment of topo-bathymetric surface models based on geospatial data recorded by UAV and USV vehicles. *Metrology and Measurement Systems*, *30*(3). 1–19. https://doi.org/10.24425/mms.2023.146421

Przemysław Pasek received his B.Sc. and M.Sc. degrees in electronics and telecommunications from the Military University of Technology in Warsaw, Poland in 2015 and 2019 respectively. Currently, pursuing his Ph.D. at the Doctoral School of the Military University of Technology, he is conducting research on position estimation algorithms designed for swarms of unmanned aerial vehicles (UAVs) as part of his doctoral dissertation. His academic interests comprise multi-sensor fusion and navigation systems, particularly focusing on data analysis algorithms for these systems.

Piotr Kaniewski studied radio systems of aircraft at the Military University of Technology in Warsaw. He graduated and received his M.Sc. in 1994, Ph.D. in 1998, and obtained his habilitation in 2011. He worked as an Engineer, Assistant, Assistant Professor, and currently works as an Associate Professor at the Faculty of Electronics of the Military University of Technology, where, since 2012, he has been the Director of the Institute of Radioelectronics. His current research is focused on navigation systems dedicated for special purposes, such as supporting synthetic aperture radars (MOCO), supporting ground penetrating radars (GPR) with accurate scanning trajectory information, distributed navigation algorithms for UAV swarms, and navigation systems for GNSS denied environments, especially using SLAM on UAVs and UWB ranging modules for indoor navigation. He is the author of more than 200 scientific papers and 2 books.